International Journal of Ambient Energy

ISSN: (Print) (Online) Journal homepage: https://www.tandfonline.com/loi/taen20

Design and analysis of a scooping engine valve

G. Boopathy, N. Ramanan & E. Gopi

To cite this article: G. Boopathy, N. Ramanan & E. Gopi (2021) Design and analysis of a scooping engine valve, International Journal of Ambient Energy, 42:4, 383-388, DOI: 10.1080/01430750.2018.1531264

To link to this article: https://doi.org/10.1080/01430750.2018.1531264

INTERNATIONAL JOURNAL OF AMBIENT ENERGY
2021, VOL. 42, NO. 4, 383–388
https://doi.org/10.1080/01430750.2018.1531264

Taylor & Francis
Taylor & Francis Group

Design and analysis of a scooping engine valve

G. Boopathy[a], N. Ramanan[b] and E. Gopi[a]

[a]Veltech Rangarajan Dr. Sagunthala R&D Institute of Technology, Chennai, India; [b]Synce Engineering Services, Chennai, India

ABSTRACT

Inlet valve in an engine tends to be subjected to immense thermal loads besides chemical corrosion. Opening and closing of inlet valve practically could be in the order of 2000 times per 1.6 km. In the mean time of engine working cycle, seat insert of the inlet valve is the surface, against which an intake valve seats. Conventional engine valves are provided with a curved angle for its seating position, but for this study, the same is proposed to be positioned at a tapered angle. This tapered position as converted into radius in order to permit rich air at the inlet and reduce exhaust emission. This study is to investigate the nature of the future redesigned Scooping valve for a 1.25L 4-cylinder Petrol engine with VTVT (Variable Timing and Valve Train) under combined mechanical and thermal loading cycle by feeding the input conditions for this study after NX-CAD modelling in ANSYS 10.0 software and the numerical results thus obtained are recorded for future valve design considerations.

ARTICLE HISTORY
Received 13 July 2018
Accepted 16 September 2018

KEYWORDS
Scooping valve; NX-CAD; ANSYS 10.0; inlet valve

1. Introduction

The inlet valve along with the seat insert is a component that is located in the cylinder head. Both works in a similar environment and also have a close relationship since both of them have to control the inflow of working fluid inside the internal combustion engine. They are intended to seal the combustion chamber against the manifold. Inlet valve is one of the precision engine components which is used to allow the working fluid into the cylinder (Weller 1993). Therefore, the inlet valve is exposed to severe thermal loads and chemical corrosion. It is a critical component so as to ensure complete sealing of the combustion chamber such that the required pressure during compression and an environment for ignition is generated inside the cylinder. Generally, the material for manufacturing inlet valve and inlet valve seat insert have properties that could withstand high operating temperature conditions throughout the functioning of the engine and exhibit resistance against corrosion from their surrounding environment in which they are to be exposed (Leskovsek 1996; Neumeier 2008). Processes involved in manufacturing these components also need high dimensional accuracy and quality heat treatment owing to severe thermal and mechanical loads (Lucchini et al. 2009). The engine valve is made up of medium carbon steel and 5 mm radius scooping position of is obtained through the EDM process.

The following data are observed from the four-stroke petrol engine:

Bore, $B = 0.08$ m
Indicated pressure, $P_m = 4\ \mathrm{MN/m^2}$
Bending stress, $\sigma_b = 46\ \mathrm{MN/m^2}$
Modulus of rigidity $= 0.48$
Angle of taper, $\Theta = 30^\circ$
Thickness of valve head, $T = \mathrm{k.\ d}\ (\sqrt{\mathrm{P}/\sigma_b})$

$$T = 0.48 \times 0.080\mathrm{x}\sqrt{(4/46)}$$
$$T = 0.011\ \mathrm{m}$$

where

$k =$ Modulus of rigidity
$d =$ diameter of the piston
$P =$ pressure of the engine valve
$\sigma_b =$ bending stress

Diameter of the stem =
Diameter of the piston/$(0.08 + 6.35)$ m

$$= 0.08/\ (8 + 6.35)$$
$$= 0.1635\ \mathrm{m}$$

Maximum lift of the valve (h) =
diameter of the piston/$4 \times \cos\Theta$

where

$\Theta =$ angle of contact of engine valve
$h = 0.080/4 \cos 30$
$h = 0.023$ m

1.1. Governing equations

Numerical analysis of the valve requires moving boundaries of the solution domain. When the mesh has moving boundaries the integral form of the conservation equation for a tensorial property, ϕ defined per unit mass in an arbitrary moving volume, V bounded by a closed surface, S (Figures 1–3).

$$\frac{\mathrm{d}}{\mathrm{d}t}\int_V \rho\varphi \mathrm{d}V + \int_S \mathrm{d}S.\rho\varphi(u - u_b) = -\oint_s \mathrm{d}S.\rho q_\varphi + \int_V S_\varphi \mathrm{d}V,$$

where p is the density, u is the fluid velocity, u_b is the boundary velocity and q_ϕ and S_ϕ are the surface and volume sources/sinks of ϕ, respectively (Dahlen 2002; Jasak 2006).

CONTACT G. Boopathy boopathyg81@gmail.com

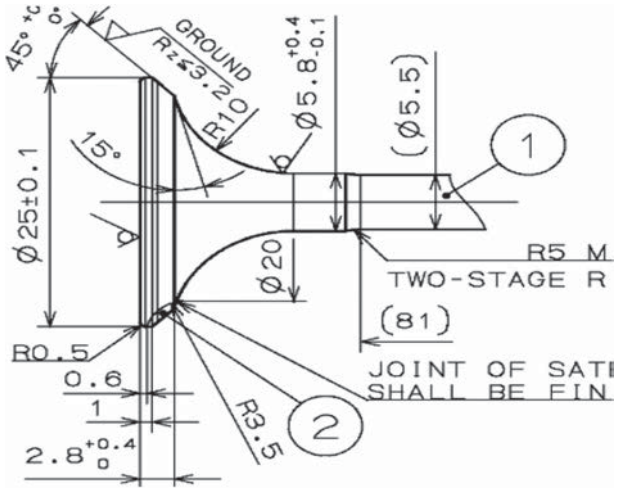

Figure 1. Inlet valve without scooping.

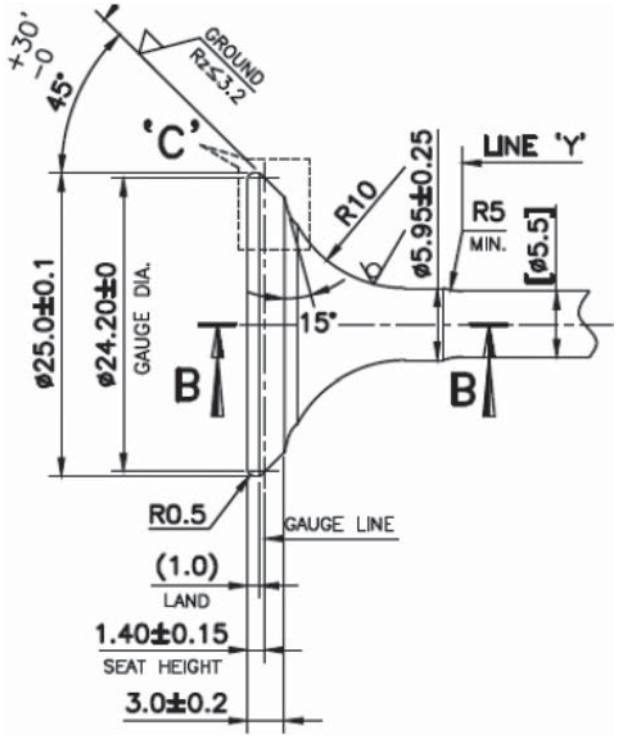

Figure 2. Inlet valve with scooping.

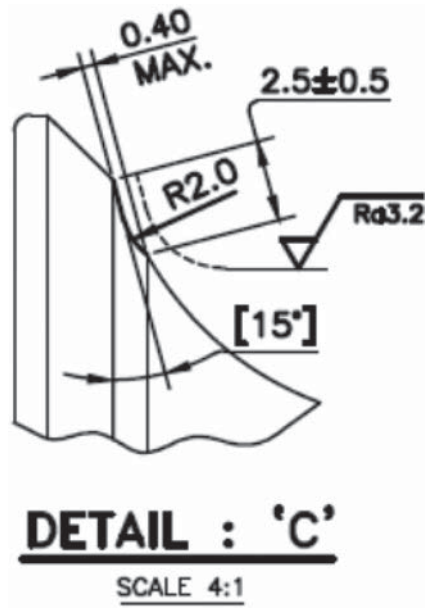

Figure 3. Scaled view of section 'C'.

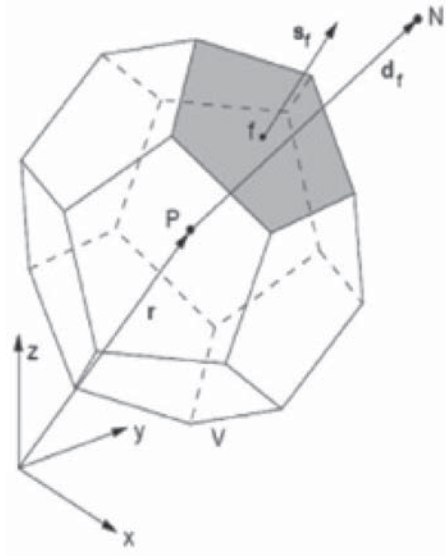

Figure 4. A polyhedral cell with fvm notations.

Since the volume V is no longer fixed in space, its motion is captured by the motion of its bounding surface S by the velocity u_b. The first term is the temporal derivative (or rate of change of $), the second is the convection term representing the convective transport by the prescribed velocity field. The third term is a diffusion term representing the gradient transport and finally, the fourth term is the source/sink term for non-transport effects, which means local production and destruction of ϕ.

1.2. Continuity equation

$$\frac{d\rho}{dt} + \nabla.(\rho u) = 0,$$

governs the conservation of mass, which means that the rate of change of mass in an arbitrary control volume must be equal to the total mass flow over the control volume boundaries.

1.3. Momentum equation

$$\frac{\partial \rho u}{\partial t} + \nabla.(\rho u u) = \rho g + \nabla.\sigma,$$

governs the conservation of linear and angular momentum. According to Newton's second law, the rate of change of momentum on a fluid particle equals the sum of forces acting on that particle.

1.4. Energy equation

$$\frac{\partial \rho h}{\partial t} + \nabla.(\rho u h) - \nabla.[(\alpha + \alpha_t)\nabla h] = Q + \frac{Dp}{dt},$$

governs the conservation of energy, where p is the density, u is the fluid flow vector, g is the body force, σ is the stress tensor, h is the enthalpy, α is the thermal diffusivity for enthalpy, α_t is the turbulent thermal diffusivity, Q is the energy source term, and p is the fluid pressure.

This equation is based on the first law of thermodynamics that says that the rate of change of total energy of a fluid element, i.e. the sum of all energy forms (internal, kinetic, mechanical, chemical, etc.) must equal the net rate of heat and work flow over its boundaries.

Unstructured FVM discretizes the computational space by splitting it into a finite number of convex polyhedral cells bounded by convex polygons which do not overlap and completely cover the solution domain (Lucchini et al. 2007; Lucchini et al. 2007). The temporal dimension is split into a finite number of time-steps and the equations are solved in a time-marching manner. A sample cell as shown in Figure 4 around the computational point, P located in its centroid, a face f, its area vector S_f and the neighbouring computational point N are shown. Second-order FV discretization transforms the surface integrals into sums of face integrals and approximates them to second order using the mid-point rule (Jasak 1996; Jasak and Tukovic 2006).

$$\frac{(\rho_P \varphi_P V_p)^n - (\rho_P \varphi_P V_P)^0}{\Delta t} + \sum_f \rho_f (F - F_S)\varphi_f = -\sum_f S_f.\rho q_\varphi + S_\varphi V_P,$$

where the subscript P represents the cell values, f the face values and superscripts n and o the 'new' and 'old' time level, VP is the cell volume, $F = S_f$-u_f is the fluid flux and Fs is the mesh motion flux. The fluid flux F is usually obtained as a part of the solution algorithm and satisfies the conservation requirements (Stralin 2007).

1.5. Pre-Processing

For this study, the T-type scooping valve along with the combustion chamber has been modelled with CATIA as shown in Figure 5.

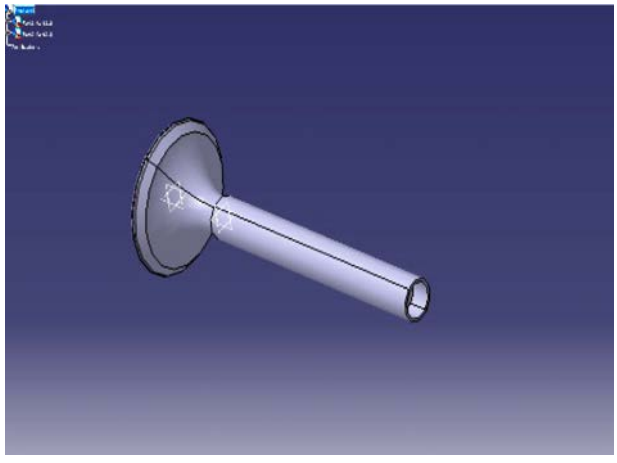

Figure 5. CATIA model of scooping valve.

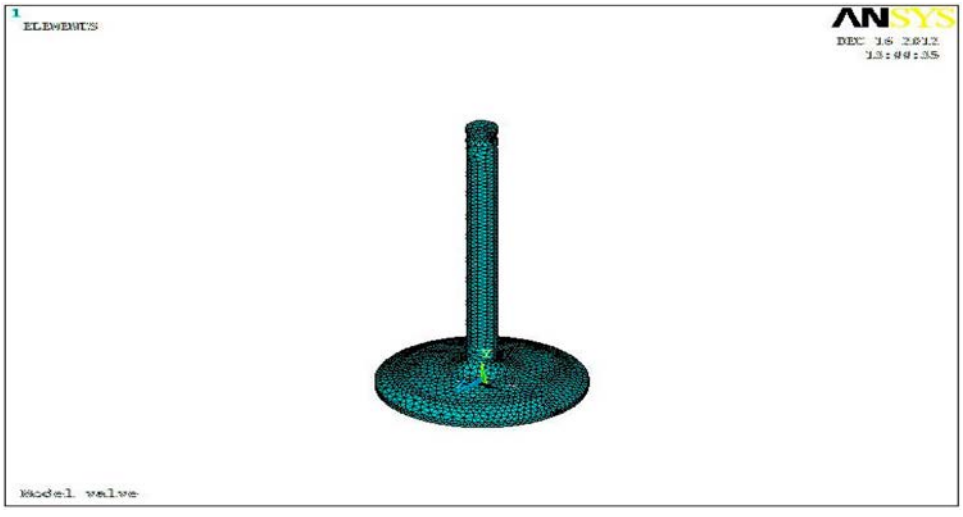

Figure 6. Meshed model of Scooping valve.

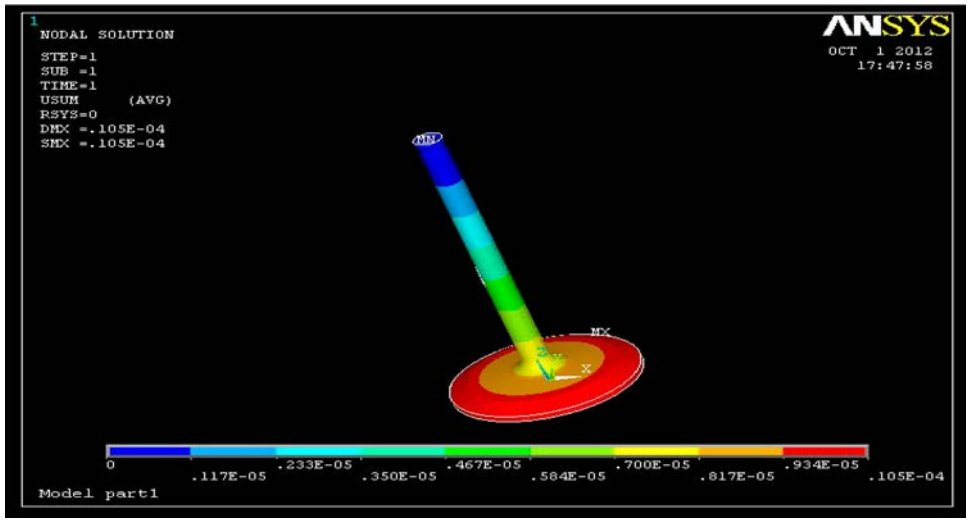

Figure 7. Post-processed result of coupled field analysis.

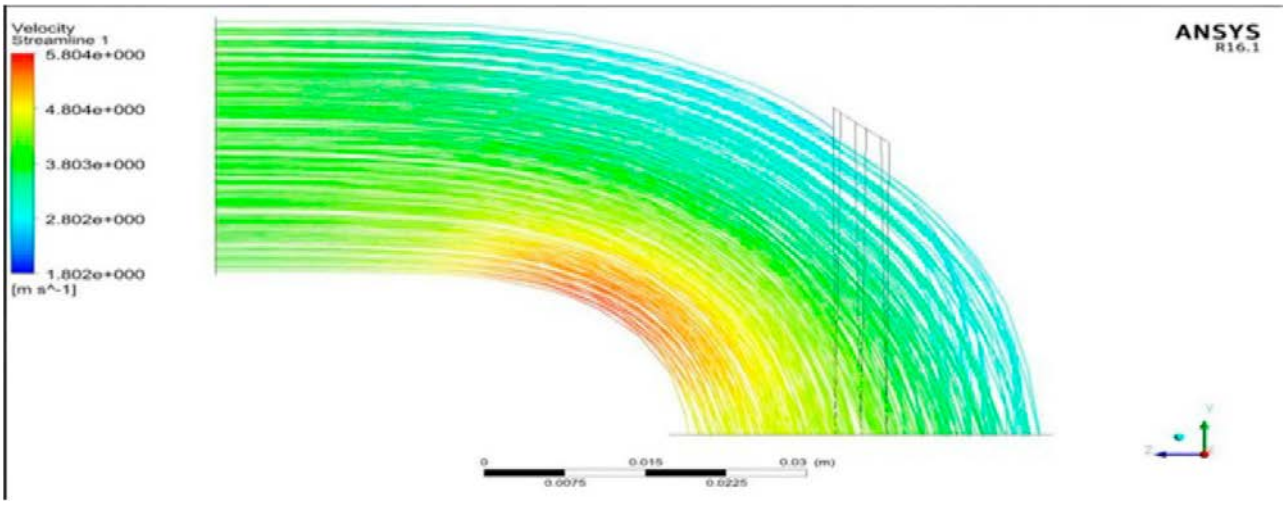

Figure 8. Air flow velocity of modify engine.

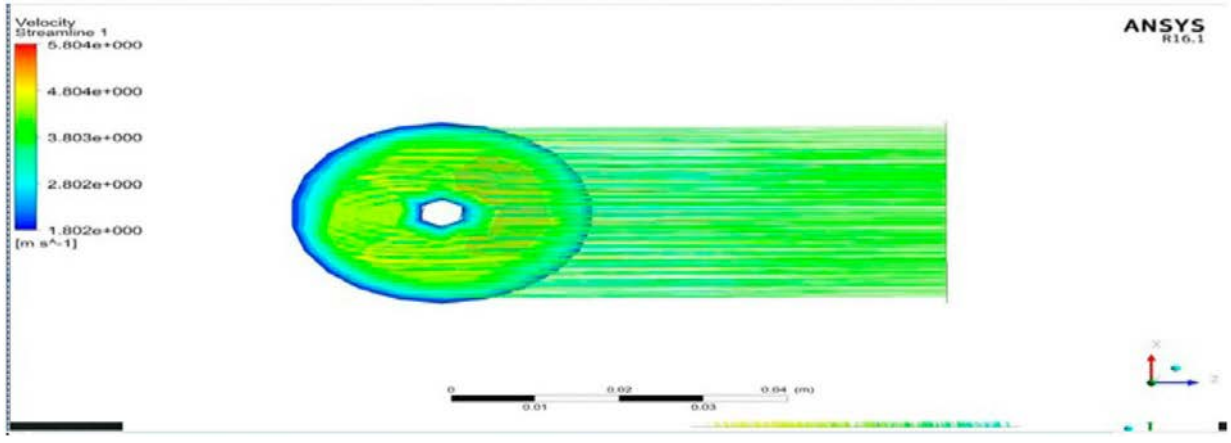

Figure 9. Air flow on engine top head on output valve.

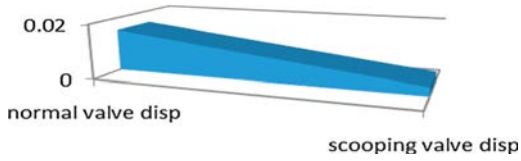

Figure 10. Comparison chart on valve displacement.

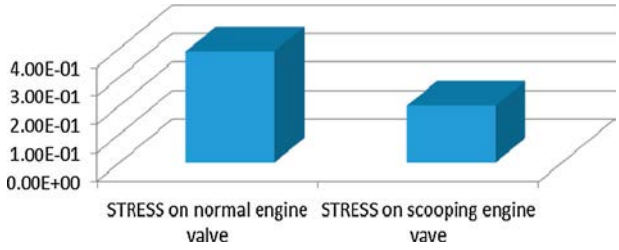

Figure 11. Comparison chart on structural stress.

1.6. Meshing

The meshed model of the above model is shown below in Figure 6.

1.7. Meshing detail

Mesh type: tetrahedral
Moving mesh: boundary velocity 120 m/s
Mesh quality check:
Aspect ratio: 0.5
Density: 5
Warpage angle: 0.2
Skew angle: 0.4

1.8. Analysis and post-processing

The meshed scooping valve model is then analyzed with ANSYS 10.0 as shown in Figure 7, with the following boundary conditions:

Inlet pressure: 4 MN/m^2
Physical and material properties:
One end fixed
One end load applied
Young's modulus and Poisson ratio as per Medium carbon steel Grade EN-32 data (Figures 7–9).

2. Result and discussions

From the above plot in Figure 10, it can be observed that the scooping engine valve displacement shows 0.0002 mm compared normal engine valve displacement 0.015 mm.

From the above plot Figure 11, it can be observed that the stress on normal engine valve 0.04 N/mm^2 and scooping engine valve 0.02 N/mm^2.

From the above plot Figure 12, it can be observed that the thermal stress of scooping engine valve 0.25 N/mm^2 compared to normal engine valve of 0.6 N/mm^2.

From the following comparison chart Figure 13, it can be observed that the air flow velocity of scooping engine valve is found to be 4.2 m/s compared to that of 6.2 m/s in the normal valve.

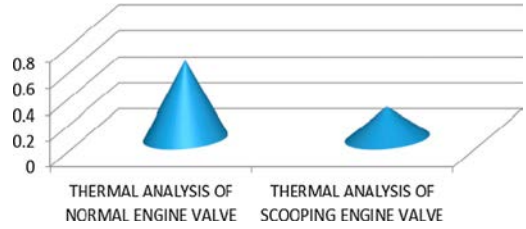

Figure 12. Comparison chart on thermal stress.

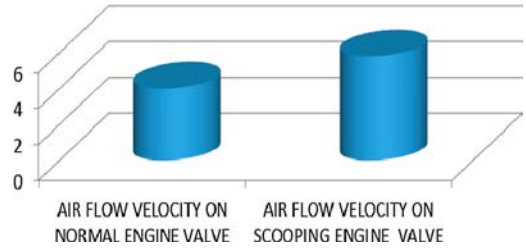

Figure 13. Comparison chart on air flow velocity at inlet.

3. Conclusion

- Throughout this study, it has been noticed that even though the profile of the valve being different from the conventional ones, there has been no major depreciation of performance characteristics.
- Thanks to the scooping in the valve, the volumetric efficiency shows marginal increase which contributes to the reduction in No_x emissions.
- Air flow velocity also has been shown an increase which is expected to be the effect of change in area cross-section across the flow.
- This in turn adds turbulence during suction and hence, increased mechanical efficiency and power output.

Disclosure statement

No potential conflict of interest was reported by the authors.

References

Dahlen, L. 2002. "On Applied CFD and Model Development in Combustion Systems Development in DI Diesel Engines: Prediction of Soot Mediated Oil Thickening." PhD thesis., Royal Institute of Technology, Stockholm.
Jasak, H. 1996. "Error Analysis and Estimation for the Finite Volume Method with Applications to Fluid Flows." PhD thesis., Imperial College of Science, Technology and Medicine, London.
Jasak, H. 2006. *Numerical Solution Algorithms for Compressible Flows*. Croatia: Faculty of Mechanical Engineering and Naval Architecture University of Zagreb.
Jasak, H., and Z. Tukovic. 2006. "Automatic Mesh Motion for the Unstructured Finite Volume Method." *Transactions of FAMENA* 30: 1–20.
Leskovsek, D. 1996. "Prediction of Combustion in Spark-Ignition Engines." PhD thesis., Imperial College of Science, Tecnology and Medicine, London.
Lucchini, T., G. D'Errico, F. Brusiani, and G. M. Bianchi. 2007. "A Finite-Element Based Mesh Motion Technique for Internal Combustion Engine Simulations." SAE Paper.

Lucchini, T., G. D'Errico, F. Brusiani, G. M. Bianchi, Z. Tukovic, and H. Jasak. 2009. "Multidimensional Modeling of the Air/Fuel Mixture Formation Process in a PFI Engine for Motorcycle Applications." SAE Paper, 2009-24-0015.

Lucchini, T., G. D'Errico, H. Jasak, and Z. Tukovic. 2007. "Automatic Mesh Motion with Topological Changes for Engine Simulation." SAE Paper, 2007-01-0170.

Neumeier, P. 2008. "In-cylinder flow modeling with OpenFOAM." Term Paper, Department of Energy, Politecnico di Milano.

Stralin, P. 2007. "Lagrangian CFD Modeling of Impinging Diesel Sprays for DIHCCI." PhD thesis., Royal Institute of Technology, Stockholm.

Weller, H. G. 1993. "The Development of a New Flame Area Combustion Model Using Conditional Averaging." Thermo-Fluids Section Report TF 9307, Imperial College of Science, Technology and Medicine.